Journal of Engineering Research and Applied Science
Available at www.journaleras.com
Volume 15 (1), June 2026, pp 77-87
ISSN 2147-3471 © 2026

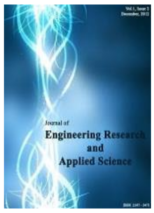

Effect of CuO Nanoparticle Size and Concentration on Thermal Enhancement in Shell-and-Tube Heat Exchangers

Gurkan Akarken[1,*], Ugur Cengiz[1,2], Tijen Ennil Bektas[2]

[1]Energy Resources Application and Research Center, Çanakkale Onsekiz Mart University, Çanakkale, Türkiye
[2]Chemical Engineering, Faculty of Engineering, Çanakkale Onsekiz Mart University, Çanakkale, Türkiye

Accepted 06 June 2026

Abstract
In this study, a custom-designed shell-and-tube heat exchanger (STHE) system was developed and initially modeled via simulation under nanoparticle-free conditions to establish baseline heat transfer parameters. Flow regimes were identified through Reynolds number calculations at different flow rates, and the corresponding convective heat transfer coefficients (hi, ho), overall heat transfer coefficient (U), and heat duty (Q) values were determined. Following simulation calibration, experimental investigations were conducted using CuO–water nanofluids with two distinct particle sizes (38 nm and 20 µm) and three concentrations (0.25%, 0.5%, and 0.75%). The impact of these parameters on the thermal performance of the STHE was evaluated under varying inlet temperature conditions. Experimental results revealed that cold fluid outlet temperatures increased significantly with the addition of nanoparticles, while hot fluid outlet temperatures decreased, indicating enhanced heat absorption. For 38 nm particles, the cold-side enhancement (ΔT) ranged from 1.0 °C to 2.2 °C, corresponding to approximately 5–12% improvement relative to the baseline. In contrast, 20 µm particles exhibited ΔT values of 1.5–2.7 °C, equating to a 6–14% increase depending on concentration and inlet temperature. The most pronounced enhancements were observed at 0.5% and 0.75% concentrations, particularly at higher temperature gradients, demonstrating that both particle size and concentration play critical roles in nanofluid-mediated heat transfer enhancement.

Keywords: *CuO nanoparticles, Heat transfer, Nanofluid, Shell and tube heat exchanger, Simulation*

1. Introduction

Rapid technological developments and increasing population have led to a continuous rise in energy demand. This situation promotes the use of fossil fuels in energy production, consequently increasing CO_2 emissions and intensifying environmental issues. In order to minimize the effects of global warming and establish a sustainable energy framework, researchers have sought innovative solutions aimed at improving energy efficiency. In this context, green chemistry practices and advanced heat transfer technologies have become significant areas of research [1-3].

The primary objective in heat transfer processes is to achieve maximum efficiency with minimum possible energy losses. However, traditional fluids possess certain physical and thermal limitations, necessitating the development of alternative solutions capable of providing more efficient heat conduction. Due to recent advances in nanotechnology, the use of nanoparticle-enhanced fluids, known as nano fluids, has come into focus to improve thermal properties of heat transfer fluids [4]. Nanofluids, which have a higher heat conduction capacity compared to conventional fluids, enhance the efficiency of heat transfer processes, significantly contributing to energy savings.

Common oxide nanoparticles in heat transfer studies include Zinc Oxide (ZnO), Copper Oxide (CuO), Aluminum Oxide (Al_2O_3), and Titanium Oxide (TiO_2), whereas metal nanoparticles include Gold (Au), Silver (Ag), and Copper (Cu) [5-8].Metal nanoparticles generally exhibit higher thermal conductivity compared to oxide nanoparticles. Metals like silver and copper particularly provide high performance in heat transfer applications [9, 10].

The synthesis of nanomaterials through hydrothermal methods can be performed over a wide temperature range, from ambient to extremely high temperatures. This method has several advantages compared to other synthesis methods. For instance, size control can be achieved by employing either low or high-pressure conditions, and the shape development of materials can be adjusted depending on the vapor pressure of the

*Corresponding author: gurkanakarken@gmail.com

primary reaction. Furthermore, hydrothermal synthesis enables the production of nanomaterials with precisely controlled compositions and can be carried out through liquid-phase or multi-step chemical process [11]. The hydrothermal method also allows for the synthesis of nanomaterials that are unstable at high temperatures. This method facilitates the production of nanomaterials under high vapor pressures, minimizing material loss during synthesis [12]. This method stands out as a suitable approach for the synthesis of copper oxide. The hydrothermal method provides nanoparticles with exceptional dispersibility, characterized by strong crystallinity, high purity, and various morphologies in different sizes [13, 14]. Recently, extensive studies have been conducted on the controlled shaping of various nanostructures. The physical and chemical properties of nanocrystals can significantly vary depending on their size, shape, composition, and structure.

Recent research has further shown that nanofluids, particularly those containing CuO, Al_2O_3, or TiO_2 particles, can substantially improve convective heat transfer in complex exchanger geometries such as shell-and-tube, twisted plate, or helically coiled systems [15-17]. In a study, conducted CFD analysis showed that Al_2O_3 and CuO nanofluids enhanced heat transfer in curved tubes, with up to 48.8% improvement at 5% concentration. Helical coils and circular sections performed best, with minimal pressure loss [18].

Besides, in the experimental study of Huseen et al., (2025) the influence of various nanomaterials specifically Al_2O_3, CuO, TiO_2, and their hybrid combinations on the thermal behavior of heat exchangers were explored [19]. The authors assessed changes in heat transfer efficiency by monitoring temperature drops and thermal conductivity in both conventional and nanomaterial-enhanced systems. Without any nanomaterials, a steady decline in temperature from 40 °C to 38.2 °C over 10 minutes was observed. However, systems incorporating TiO_2 and Al_2O_3–CuO hybrids exhibited significantly improved cooling performance, with outlet temperatures reduced to as low as 34.8 °C, depending on the composition. Among these, hybrid nanofluids containing Al_2O_3 and CuO offered superior thermal conductivity and enhanced heat removal due to their synergistic interaction, resulting in a more efficient heat exchange process. In another study Norouzi et al., (2023), authors demonstrates that CuO/water and Al_2O_3/water nanofluids significantly improve the thermal output of abandoned oil wells repurposed for seawater desalination [20]. Using a coaxial borehole heat exchanger and advanced thermal insulation, the system achieved a 14% and 12.9% increase in fluid temperature, respectively, over pure water.

The heat transfer performance of Al_2O_3 and CuO nanofluids in helical coil heat exchangers were investigated in a recent study. Results show that increasing nanoparticle concentration significantly improves thermal conductivity and convective heat transfer, leading to a 38.8% enhancement in exchanger efficiency compared to water [19]. The thermal performance of U-type tubular heat exchangers (HEXs) using CuO-Al_2O_3/water hybrid nanofluids through both experimental and numerical analyses were also explored in another study. Compared to single nanofluids and water, hybrid nanofluids enhanced the overall heat transfer coefficient by up to 12%, demonstrating their effectiveness in improving HEX efficiency [20]. In the study of Naseema, et al., (2018) thermal performance of Al_2O_3 and CuO nanofluids at varying volume concentrations (0.1%, 0.25%, and 0.4%) in turbulent flow regimes was investigated the. Results show that incorporating these nanoparticles into conventional fluids enhances heat transfer significantly, highlighting their potential for use in compact heat exchangers and advanced thermal systems [21].

The most important element in heat exchanger systems is the working fluid. In these systems, to enhance efficiency, it is desirable that the heat transfer coefficient of the secondary fluid, used for heating or cooling the primary fluid, is high [22]. A low heat transfer coefficient decreases overall efficiency. For this purpose, obtaining novel and economically feasible fluids is a significant and contemporary topic.

In this study, the thermal performance of nanofluids containing CuO (Copper (II) Oxide) nanoparticles at different particle sizes (38 nm and 20 µm) and concentrations (0.25%, 0.5%, and 0.75%) were experimentally investigated in a 2-pass shell-and-tube heat exchanger. The study aims to clarify how nanoparticle dimensions and temperature affect the heat transfer efficiency [16, 23].

2. Material and Method

A shell-and-tube heat exchanger was custom-designed and installed in our laboratory (Figure 1). This device consists of 32 stainless steel tubes (SS-304), each with an 8×10 mm cross-section and a length of 1 meter, arranged in a U-type configuration with 16 forward and 16 return passes. The tubes are positioned with a 60° angular layout and a 12.5 mm spacing between them to promote uniform flow and turbulence. The outer shell is constructed from stainless steel with an internal diameter of 100 mm. To enhance thermal performance and control flow direction, the shell includes 10 baffle plates, each with a 32% cut-out ratio.

The overall experimental setup, including the heating and cooling subsystems, fluid circulation components, and measurement instruments, is illustrated in Figure 2. This flow schematic outlines the closed-loop system comprising nanofluid and water circuits, equipped with flowmeters, temperature indicators, pumps, a heating tank, and a nanofluid reservoir. Reflux lines are incorporated to regulate flow stability, and precise temperature monitoring at four critical points (T1–T4) ensures accurate data collection. This configuration enables comprehensive thermal performance evaluation under varying operational conditions and nanoparticle concentrations.

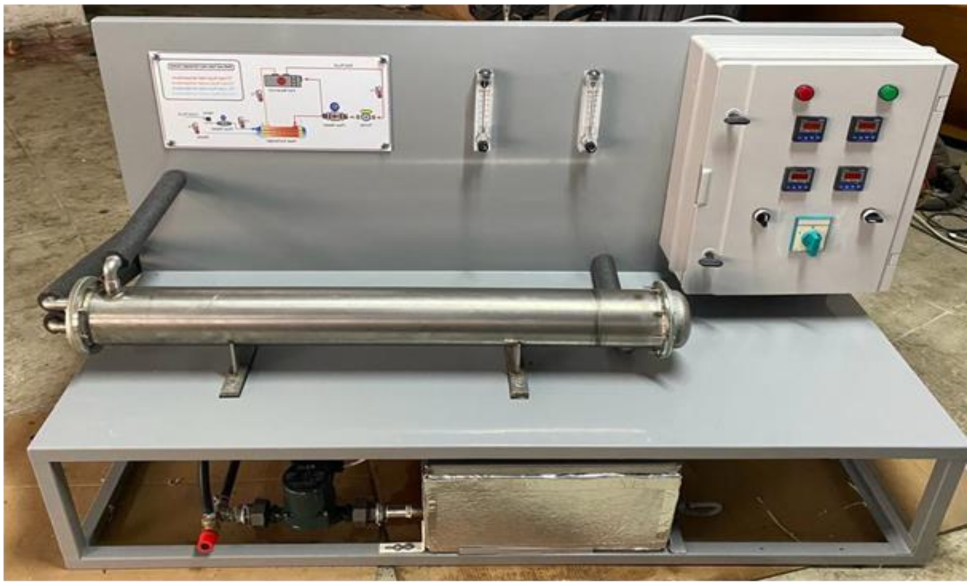

Figure 1. Schematic view of the custom-designed 2-pass shell-and-tube heat exchanger system

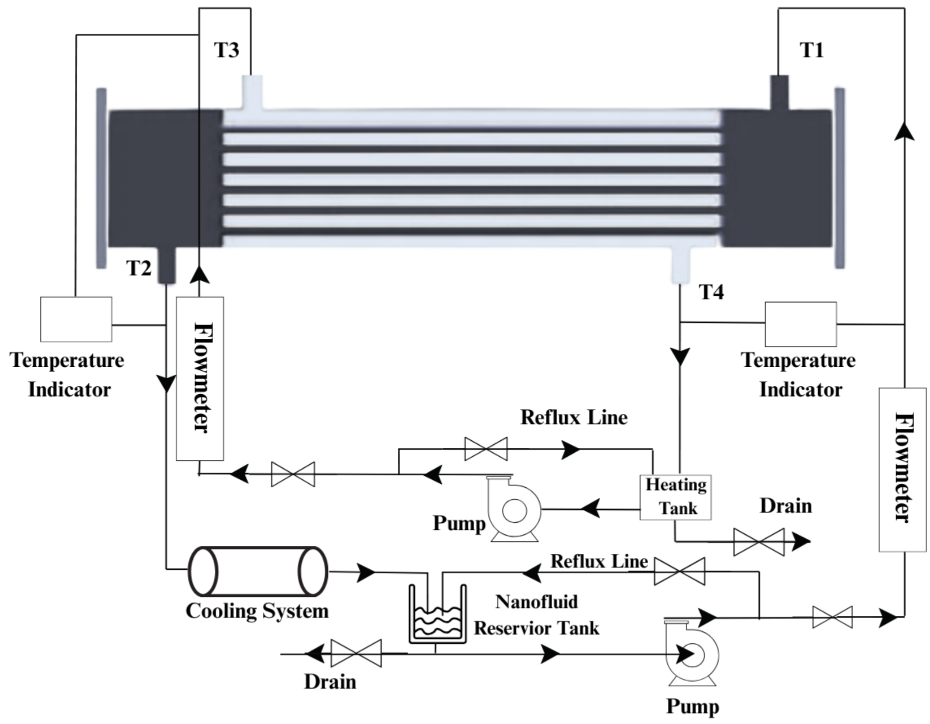

Figure 1. Experimental flow schematic of the nanofluid-based shell-and-tube heat exchanger test system including heating, cooling, and circulation loops

In this study, CuO nanoparticles with varying particle sizes were synthesized by altering reaction temperature and duration [24]. The particle dimensions within the samples were analyzed using a JEOL JEM-1400 transmission electron microscope (TEM). To obtain high-quality TEM micrographs, the synthesized nanoparticles were thoroughly purified through repeated washing with ethanol and distilled water. The particles were then manually ground with a mortar to achieve a finer size suitable for imaging. Due to the intrinsic conductivity of CuO nanoparticles, no additional conductive coating was required. Particle size distributions at the nanoscale were determined by analyzing the TEM micrographs.

As shown in the TEM image (Figure 3), the nanoparticles predominantly exhibit spherical or slightly irregular shapes. The particles display well-defined crystalline structures, with sizes ranging from approximately 32 nm to 40 nm, and an average size of around 38 nm. These values are consistent with previously reported results for CuO nanoparticles synthesized through similar methods [25, 26]. Some degree of agglomeration was observed, which is commonly attributed to the high surface energy of nanoparticles, often leading to clustering during synthesis or drying [27]. Nevertheless, the overall particle size distribution remained relatively uniform, indicating effective control over synthesis conditions.

In addition to the spherical particles, a few rod-like or sheet-like structures were occasionally identified. These may result from anisotropic growth mechanisms influenced by specific synthesis parameters. However, such morphologies were infrequent and did not represent the dominant particle population. The results confirm the successful synthesis of CuO nanoparticles with controlled morphology and size. These nanoparticles with different sizes were subsequently tested in the heat exchanger to investigate the effect of nanoparticle diameter and concentration on thermal conductivity.

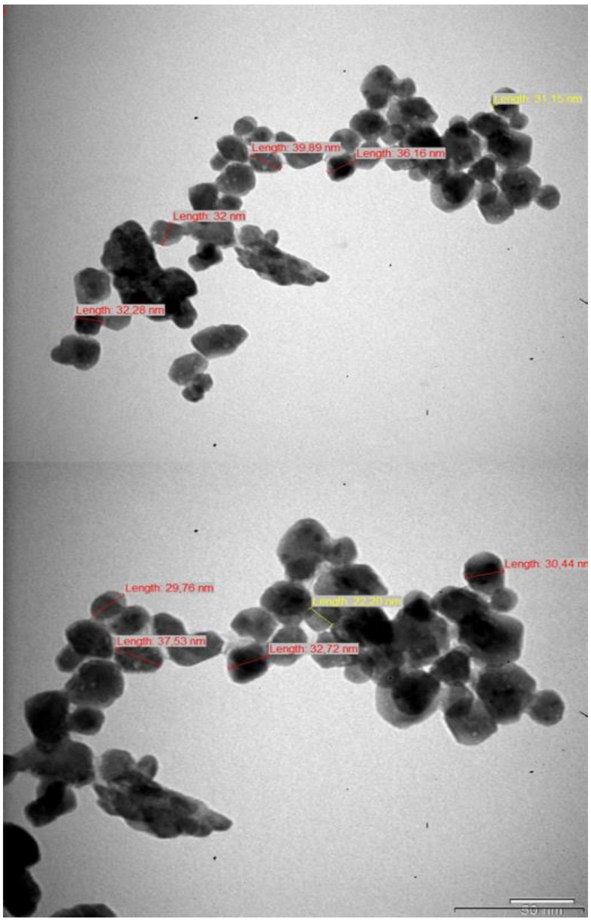

Figure 3. TEM images of CuO nanoparticles

3. Results and Discussion

In line with the technical data of the described shell-and-tube heat exchanger, a simulation model was created, and the performance analysis of the system was conducted. Within the simulation scope, flow characteristics were specifically examined for various flow rates on the tube side, the Reynolds number was calculated accordingly, and convection coefficients were determined (Table 1). As observed in Table 1, when operated at volumetric flow rates between 5–15 L/min, convection coefficients ranged from 1050 to 3600, indicating a transition from laminar (Re = 1960) to turbulent flow conditions (Re = 5723).

Simulation studies without nanoparticles were conducted to determine appropriate flow regimes and baseline thermal performance parameters such as heat transfer rate (Q) and overall heat transfer coefficient (U). These baseline results were then used as a reference to evaluate the enhancement effects of nanofluids by comparing them with experimental data obtained using CuO based nanofluids under similar operating conditions.

Table 1. Simulation study results of shell-and-tube heat exchanger in the absence of nanofluid

Run	Tci/Thi °C	qi/qo L/min	Tco/Tho °C	Re_c/Re_h	Hi/Ho W/m²·K	U W/m²·K	Q kJ/s	LMTD °C
Run 1	25/50	(15/7)	29.1 /41.2	5632 / 350	3605 / 928	527	4.24	18.32
Run 2	25/50	(10/7)	30.6 /41.8	3813 / 353	2484 / 948	493	3.85	18.17
Run 3	25/50	(7/7)	31.7 /42.9	2702 / 340	1405 / 951	414	3.28	18.14
Run 4	25/50	(5/7)	33.3/44.0	1960 / 343	1051 / 960	374	2.864	17.81
Run 5	25/50	(15/15)	30.7 / 44.3	5723 / 817	3633 / 1606	695	5.92	19.3
Run 6	25/50	(10/5)	30 / 40.0	2470 / 237	3795 / 829	458	3.47	17.43
Run 7	25/50	(7/15)	33.6 / 46.0	2752 / 830	1448 / 1646	515	4.21	18.6
Run 8	25/50	(5/15)	35.1 / 46.6	1996 / 835	1075 / 1661	447	3.54	18

The simulation study was conducted for a shell-and-tube heat exchanger in the absence of nanofluids (Table 1), where the cold fluid flows through the tubes and the hot fluid flows through the shell side. As observed in the table, various combinations of cold and hot fluid flow rates were tested while maintaining a constant inlet temperature difference of 25°C (25°C for cold inlet and 50°C for hot inlet). The performance parameters such as overall heat transfer coefficient (U), heat transfer rate (Q), and logarithmic mean temperature difference (LMTD) were evaluated. Among the trials, Run 5 (with equal flow rates of 15 L/min on both sides) exhibited the highest heat transfer rate (Q = 5.92 kJ/s) and the maximum overall heat transfer coefficient (U = 695 W/m²·K), indicating an optimal balance between convective heat transfer and flow rate. Conversely, Run 8 showed the lowest thermal performance, associated with a lower cold fluid flow rate (5 L/min), despite having a high LMTD. The results demonstrate that increasing cold fluid flow rate in the tube side significantly enhances the thermal performance of the heat exchanger under these specific operating conditions.

The data presented in Table 1 represent the baseline calibration results of the system under conditions without any nanofluid present. These findings were then used with experimental results to better understand the effect of nanofluids on heat transfer performance and to evaluate overall system efficiency (Table 2).

Table 2 includes experiments designed for various nanofluid diameters and concentrations (especially hot and cold fluid inlet temperatures are also variable here).

A comprehensive experimental design was implemented to evaluate the combined effects of nanoparticle size, concentration, and inlet temperatures on the thermal performance of a shell-and-tube heat exchanger. The study employed CuO nanofluids with two particle sizes (38 nm and 20 µm) and three concentration levels (0.25%, 0.5%, and 0.75% vol.). In addition to nanoparticle parameters, the inlet temperatures of both hot (Thi = 40–60°C) and cold (Tci) streams were systematically varied. This multi-variable design allowed for the examination of not only the individual effects of nanoparticle features but also their interaction with temperature gradients.

The comparison of experimental and simulation outlet temperature data for cold and hot flows at different particle sizes is presented in Figures 4-7. Figure 4 shows the outlet temperature of the cold fluid obtained from both simulation (Tco/S) and experimental (Tco/E) data using 38 nm CuO nanoparticles at different inlet temperatures and concentrations.

The effect of 38 nm nanoparticles on the thermal performance of the heat exchanger was evaluated by comparing experimental results, obtained using nanofluids at various concentrations, with baseline simulation data representing conditions without nanoparticles. As illustrated in Figure 4a, the outlet temperature of the cold fluid (Tco) consistently increased in the presence of nanoparticles across all test runs, indicating enhanced heat absorption. The difference between experimental and simulated outlet temperatures (Figure 4b) further quantifies this improvement, with temperature gains ranging from approximately 1.0°C to 2.2°C. These enhancements are attributed to the increased thermal conductivity and improved convective heat transfer properties introduced by the suspended nanoparticles. The highest temperature rise was observed in Run 6 and Run 9, suggesting that both nanoparticle concentration and inlet temperature significantly influence the thermal performance. Overall, the results confirm the effectiveness of nanofluids in boosting the heat transfer capability of conventional systems under varying operational conditions.

Table 2. Experimental conditions for nanofluid-based heat transfer experiments

Run	Nano	Cons. (%)	Thi (°C)	Tci (°C)
1	38nm	0.25	40	34.4
2	38nm	0.25	50	42.2
3	38nm	0.25	60	49.6
4	38nm	0.5	40	33
5	38nm	0.5	50	39.9
6	38nm	0.5	60	46.6
7	38nm	0.75	40	33
8	38nm	0.75	50	40.3
9	38nm	0.75	60	47.2
10	20μm	0.25	40	33.5
11	20μm	0.25	50	40.7
12	20μm	0.25	60	46.7
13	20μm	0.5	40	33.2
14	20μm	0.5	50	40.1
15	20μm	0.5	60	47.3
16	20μm	0.75	40	34.4
17	20μm	0.75	50	42
18	20μm	0.75	60	50.1

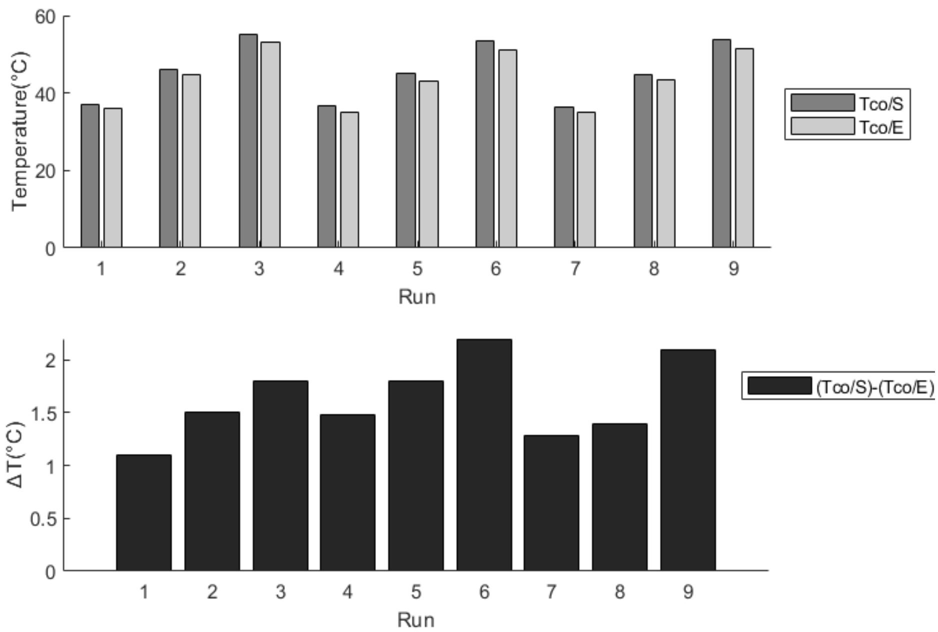

Figure 4. Change in the outlet temperature of the cold fluid under different inlet temperature conditions when using 38 nm nanoparticles at different concentrations a) simulation vs. experimental results b) difference graph

The influence of nanoparticle concentration on the enhancement of cold fluid outlet temperature was evident across the experimental runs. As the nanoparticle concentration increased from 0.25% to 0.75%, the temperature gain ($\Delta T = T_{co/E} - T_{co/S}$) also increased, confirming the role of nanoparticles in improving heat transfer. Runs with 0.25% concentration showed a modest temperature increase (approximately 1.0–1.5°C), while those with 0.75% concentration demonstrated the most significant enhancement (up to 2.2°C). However, the relationship between concentration and thermal improvement was not strictly linear. The results suggest that beyond a certain point, additional concentration yields diminishing returns, possibly due to increased viscosity and particle agglomeration. Furthermore, the combined effects of inlet temperature and concentration appear to synergistically influence performance, as the highest gains occurred in runs with both elevated concentrations and inlet temperatures.

Figure 5 presents the outlet temperature of the hot fluid using 38 nm CuO nanoparticles, comparing simulation (Tho/S) and experimental (Tho/E) results. Similarly, on the hot fluid side (Figure 5), a consistent decrease in outlet temperature was observed in the presence of nanoparticles compared to the base case. This confirms enhanced heat extraction by the nanofluid, aligning well with the increased outlet temperatures of the cold fluid. The largest differences were again observed in Runs 6 and 9, reinforcing the combined influence of nanoparticle concentration and thermal gradient on overall heat transfer efficiency.

The influence of nanoparticle concentration on heat transfer enhancement was further examined using 20 µm particles across Runs 10–18 (Figure 6). A clear trend emerged in which increasing particle concentration led to higher cold fluid outlet temperatures, with the temperature difference ($T_{co/E} - T_{co/S}$) ranging from approximately 1.5°C at 0.25% concentration to 2.7°C at 0.75%. This suggests that even relatively large particles can significantly improve thermal performance when properly suspended and distributed in the fluid. The highest improvements were observed in Runs 12 and 15, both corresponding to the highest concentration level, indicating that concentration is a dominant factor in enhancing convective heat transfer. Notably, despite their lower surface-area-to-volume ratio compared to nanoscale particles, the 20 µm particles demonstrated comparable or superior thermal effects under these conditions. This can be attributed to reduced interfacial resistance and favorable flow dynamics, particularly in systems where sedimentation and aggregation are minimized. Overall, the results confirm that optimizing particle size and concentration in tandem can yield substantial gains in heat exchanger efficiency.

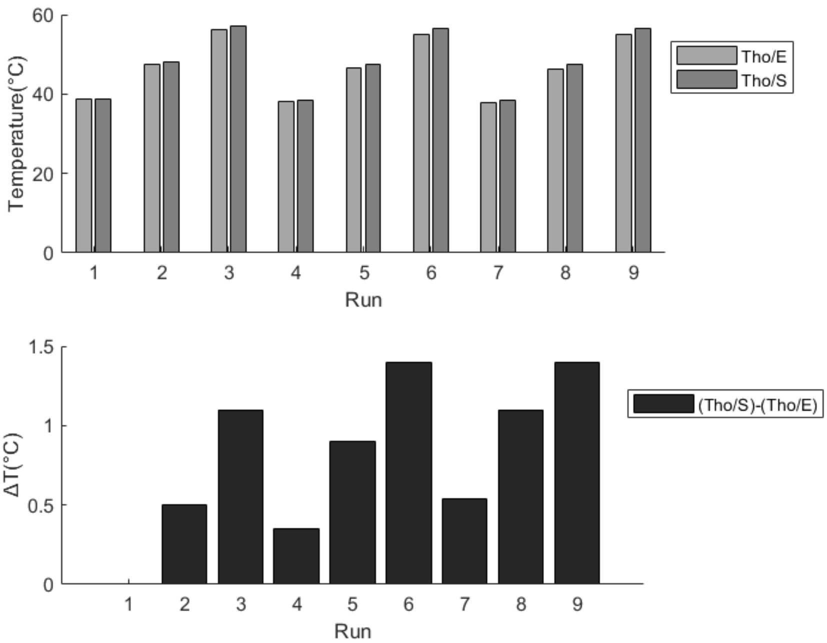

Figure 5. Change in the outlet temperature of the hot fluid under different inlet temperature conditions when using 38 nm nanoparticles at different concentrations a) simulation vs. experimental results b) difference graph

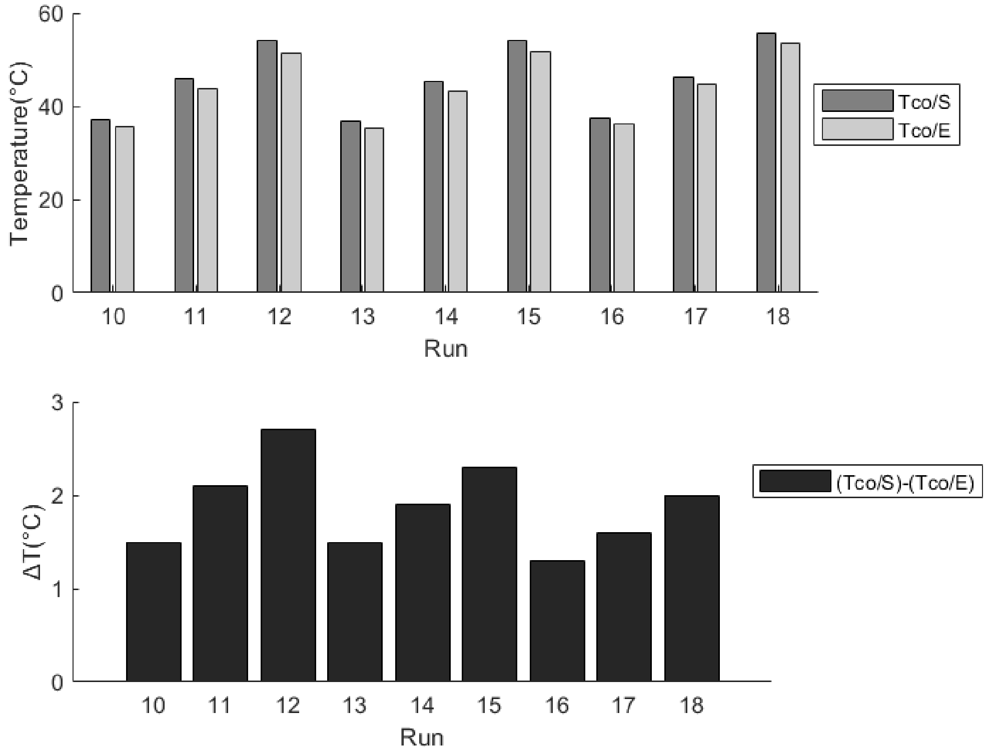

Figure 6. Change in the outlet temperature of the cold fluid under different inlet temperature conditions when using 20 μm nanoparticles at different concentrations a) simulation vs. experimental results b) temperature difference graph

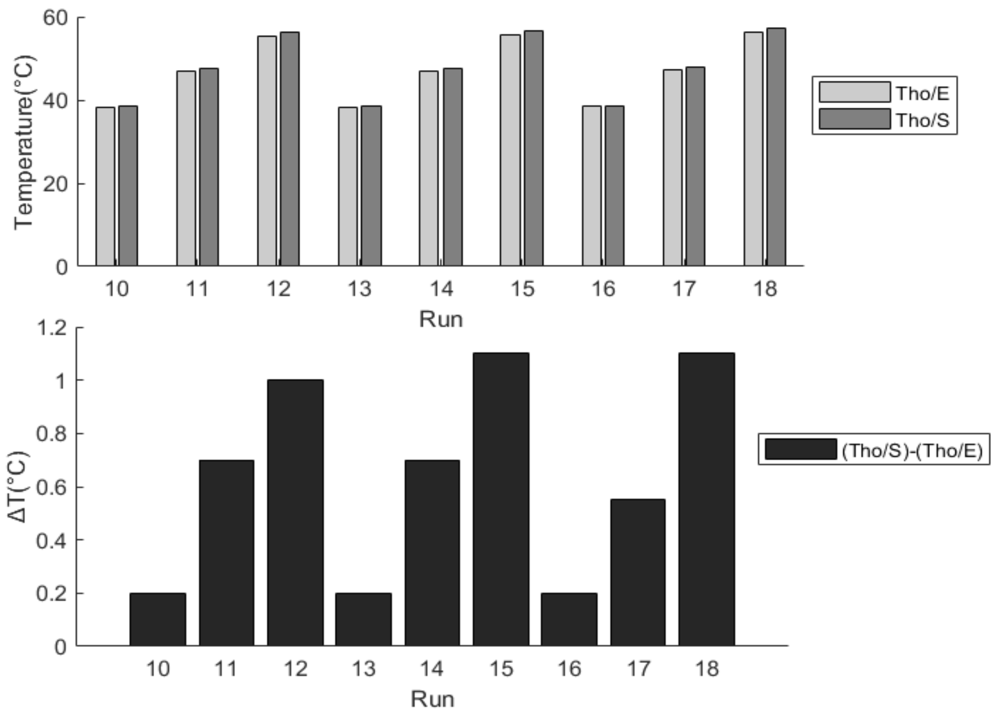

Figure 7. Change in the outlet temperature of the hot fluid under different inlet temperature conditions when using 20 μm nanoparticles at different concentrations a) simulation vs. experimental results b) temperature difference graph

Figure 6 shows simulation (Tco/S) and experimental (Tco/E) outlet temperatures for the cold fluid with 20 µm CuO particles.

Figure 7 compares the outlet temperature of the hot fluid for 20 µm CuO nanofluids, as obtained from simulation (Tho/S) and experimental (Tho/E) data.

The thermal response of the hot fluid under the influence of 20 µm particles is presented in Figure 7. In all runs, the outlet temperature of the hot fluid (Tho) was lower in the presence of microparticles compared to the simulation baseline, indicating effective heat removal by the nanofluid. The temperature difference (Tho/S − Tho/E) ranged from approximately 0.2°C to 1.1°C, with the greatest reductions observed in Runs 15 and 18. These findings align with the corresponding increases in cold fluid outlet temperature reported in Figure 6, confirming the overall enhancement in heat transfer. The parallel behavior between hot and cold sides again highlights the significant role of particle concentration, with the largest thermal effects appearing at 0.75% loading. Although the heat extraction effect was slightly lower than that observed with 38 nm particles, the performance of 20 µm particles remained notable, particularly under optimized flow conditions. These results suggest that microscale particles, when stabilized and well-dispersed, can serve as viable alternatives in heat exchanger systems, balancing thermal performance with cost and handling advantages.

The inlet temperature of the hot fluid was found to play a significant role in determining the extent of heat transfer enhancement achieved with nanofluids. Runs conducted under higher inlet temperature conditions, such as Run 6 and Run 9, exhibited the greatest increase in cold fluid outlet temperature compared to the baseline (up to 2.2°C), indicating a stronger nanoparticle-induced enhancement. This can be attributed to the fact that a greater temperature gradient between hot and cold fluids facilitates more effective heat exchange, thereby amplifying the influence of the nanoparticles' superior thermal conductivity. Additionally, higher temperatures may improve the dispersion and mobility of nanoparticles, further boosting convective heat transfer. In contrast, lower inlet temperatures (e.g., Run 1 and Run 7) resulted in modest improvements (~1.0–1.3°C), reinforcing the importance of thermal driving force in maximizing the benefit of nanofluid applications.

A comparative analysis of average temperature differences for both cold and hot fluids reveal distinct performance trends based on particle size and concentration. For 38 nm particles, the cold-side heat transfer improvement increased with concentration up to 0.50%, after which a slight decline was observed suggesting an optimal concentration threshold. In contrast, 20 µm particles exhibited the highest cold-side enhancement at the lowest concentration (2.10°C at 0.25%), with decreasing effectiveness at higher loadings. This behavior may be attributed to sedimentation and flow resistance effects that become significant at elevated concentrations for larger particles. When comparing particle sizes at equal concentrations, microparticles outperformed nanoparticles at low and moderate concentrations but fell behind at 0.75%. These results highlight the complex interplay between particle size, concentration, and flow behavior, underscoring the need for tailored optimization in nanofluid-based heat exchanger applications.

4. Conclusions

In this study, the thermal performance of a custom-built shell-and-tube heat exchanger (STHE) was investigated through both simulation and experimental methods, with a focus on the influence of CuO nanoparticle size and concentration. The baseline performance of the STHE system was first established via simulations without nanoparticles, enabling the determination of flow regimes, convective heat transfer coefficients, and overall heat transfer coefficients (U). These simulations revealed that increasing the flow rate of the cold fluid significantly improved system performance, with the highest heat duty and U value recorded at balanced flow rates on both sides of the exchanger. Following simulation validation, a series of experimental tests were conducted using CuO–water nanofluids at two particle sizes: 38 nm (nanoscale) and 20 µm (microscale) and three volumetric concentrations (0.25%, 0.5%, 0.75%). Comparative analysis of cold and hot fluid outlet temperatures between simulations and experiments demonstrated that the introduction of nanoparticles substantially enhanced heat transfer. For 38 nm particles, temperature gains on the cold side ranged from 1.0 °C to 2.2 °C, while 20 µm particles yielded even higher improvements in some cases, ranging from 1.5 °C to 2.7 °C. These correspond to average thermal enhancements of approximately 5–14% over the nanoparticle-free baseline, depending on concentration and inlet temperature. Notably, the highest gains were observed at elevated inlet temperatures (Thi = 60°C), where thermal gradients were maximized. This confirmed that the effectiveness of nanofluids is further amplified under conditions of high driving force. For 38 nm particles, performance increased with concentration up to 0.5%, after which a slight decline was observed likely due to increased viscosity and potential nanoparticle agglomeration. On the other hand, 20 µm particles exhibited peak performance at 0.25% concentration, with diminishing returns at higher concentrations, possibly due to sedimentation and reduced stability.

From a design perspective, the findings underscore the importance of optimizing both nanoparticle size and concentration based on specific thermal and flow conditions. While nanoscale particles provide more predictable enhancement trends, microscale particles may offer comparable or superior performance under certain flow regimes, with advantages in cost and handling. Overall, this study highlights the potential of CuO-based nanofluids to significantly improve the heat transfer efficiency of shell-and-tube heat exchangers and provides valuable insight into the operational parameters necessary to maximize such benefits.

Acknowledgement
This work was supported by the Office of Scientific Research Projects Coordination at Çanakkale Onsekiz Mart University, Grand number: FBA-2022-4212. The authors would like to thank Central Laboratory of Çanakkale Onsekiz Mart University for providing TEM.

Author contribution
Gurkan Akarken: Conceptualization, experimental work, data analysis, manuscript writing.
Ugur Cengiz: Supervision, methodological guidance, manuscript review.
Tijen Ennil Bektas: Experimental support, data validation, manuscript review.

Declaration of ethical code
The authors of this article declare that the materials and methods used in this study do not require ethics committee approval and/or legal-special permission.

Conflicts of interest
The authors declare that there is no conflict of interest.

References
[1]. Aras, O., & Bayramoğlu, M. (2012). A MINLP study on shell and tube heat exchanger: Hybrid branch and bound/meta-heuristics approaches. *Industrial & Engineering Chemistry Research*, 51(43), 14158–14170. https://doi.org/10.1021/ie3011462
[2]. Fang, B., Tan, Y., Li, C., Cao, Y., Liu, J., Schweizer, P. J., Shi, H., Zhou, B., Chen, H., & Hu, Z. (2016). Energy sustainability under the framework of telecoupling. *Energy*, 106, 253–259. https://doi.org/10.1016/j.energy.2016.03.055
[3]. Chen, P., Wu, Y., Meng, J., He, P., Li, D., Coffman, D. M., & Guan, D. (2022). The heterogeneous role of energy policies in the energy transition of Asia–Pacific emerging economies. *Nature Energy*, 7(7), 588–596. https://doi.org/10.1038/s41560-022-01029-2
[4]. Rostami, S., Nadooshan, A. A., Raisi, A., & Bayareh, M. (2021). Modeling the thermal conductivity ratio of an antifreeze-based hybrid nanofluid containing graphene oxide and copper oxide for use in thermal systems. *Journal of Materials Research and Technology*, 11, 2294–2304. https://doi.org/10.1016/j.jmrt.2021.02.044
[5]. Hu, X. L., Zhang, T., Chen, J., Gao, H., & Cai, W. (2016). Novel synthesis of CuO nanofiber balls and films and their UV–visible light filtration property. *Ceramics International*, 42(7), 8505–8512. https://doi.org/10.1016/j.ceramint.2016.02.076
[6]. Sözen, A., Variyenli, H. I., Özdemir, M. B., Guru, M., & Aytac, I. (2016). Heat transfer enhancement using alumina and fly ash nanofluids in parallel and cross-flow concentric tube heat exchangers. *Journal of the Energy Institute*, 89(3), 414–424. https://doi.org/10.1016/j.joei.2015.02.012
[7]. Feng, L., Wang, R., Zhang, Y., Ji, S., Chuan, Y., Zhang, W., Liu, B., Yuan, C., & Du, C. (2019). In situ XRD observation of CuO anode phase conversion in lithium-ion batteries. *Journal of Materials Science*, 54(2), 1520–1528. https://doi.org/10.1007/s10853-018-2885-0
[8]. Aytac, I. (2021). Investigation of the effect of CuO/water and ZnO/water nanofluids on heat pipe performance. *Journal of Polytechnic*, 24(3), 963–971. https://doi.org/10.2339/politeknik.755358
[9]. Kulkarni, D. P., Das, D. K., & Vajjha, R. S. (2009). Application of nanofluids in heating buildings and reducing pollution. *Applied Energy*, 86(12), 2566–2573. https://doi.org/10.1016/j.apenergy.2009.03.021
[10]. Afsharpanah, F., Mousavi Ajarostaghi, S. S., Hamedani, F. A., & Pour, M. S. (2022). Compound heat transfer augmentation of a shell-and-coil ice storage unit with metal-oxide nano additives and connecting plates. *Nanomaterials*, 12(6), 1027. https://doi.org/10.3390/nano12061010
[11]. Basnet, P., & Chatterjee, S. (2020). Structure-directing property and growth mechanism induced by

capping agents in nanostructured ZnO during hydrothermal synthesis—A systematic review. *Nano-Structures & Nano-Objects,* 22, 100426. https://doi.org/10.1016/j.nanoso.2020.100426

[12]. Gan, Y. X., Jayatissa, A. H., Yu, Z., Chen, X., & Li, M. (2020). Hydrothermal synthesis of nanomaterials. *Journal of Nanomaterials*, 2020, Article 8917013. https://doi.org/10.1155/2020/8917013

[13]. Shi, W. D., Song, S. Y., & Zhang, H. J. (2013). Hydrothermal synthetic strategies of inorganic semiconducting nanostructures. *Chemical Society Reviews*, 42(13), 5714–5743. https://doi.org/10.1039/C3CS60070F

[14]. Yang, Q., Lu, Z., Liu, J., Lei, X., Chang, Z., Luo, L., & Sun, X. (2013). Metal oxide and hydroxide nanoarrays: Hydrothermal synthesis and applications as supercapacitors and nanocatalysts. *Progress in Natural Science: Materials International*, 23(4), 351–366. https://doi.org/10.1016/j.pnsc.2013.06.015

[15]. Qi, C., Luo, T., Liu, M., Fan, F., & Yan, Y. (2019). Experimental study on the flow and heat transfer characteristics of nanofluids in double-tube heat exchangers based on thermal efficiency assessment. *Energy Conversion and Management,* 197, 111877. https://doi.org/10.1016/j.enconman.2019.111877

[16]. Zolghadri, A., Maddah, H., Ahmadi, M. H., & Sharifpur, M. (2021). Predicting parameters of heat transfer in a shell and tube heat exchanger using aluminum oxide nanofluid with artificial neural network and self-organizing map. *Sustainability,* 13(16), 9147. https://doi.org/10.3390/su13168824

[17]. Colak, A. B., Akgul, D., Mercan, H., Dalkilic, A. S., & Wongwises, S. (2023). Estimation of heat transfer parameters of shell and helically coiled tube heat exchangers by machine learning. *Case Studies in Thermal Engineering,* 42, 102734. https://doi.org/10.1016/j.csite.2023.102713

[18]. Abdelmagied, M. (2025). Numerical analysis on heat transfer enhancement of Al_2O_3 and CuO–water nanofluids in annular curved tubes. *International Journal of Air-Conditioning and Refrigeration*, 33(1), 1–10. https://doi.org/10.1007/s44189-024-00066-8

[19]. Huseen, H., Jurmut, H. A., & Nasir, K. F. (2025). An experimental study on the effect of nanomaterials, hybrid nanomaterials, and composite nanomaterials on heat exchangers. *Journal of Advanced Research in Fluid Mechanics and Thermal Sciences*, 128(2), 33–50. https://doi.org/10.37934/arfmts.128.2.3350

[20]. Norouzi, M., Rashidi, F., Noorollahi, Y., & Qom, H. F. (2023). CuO/water and Al_2O_3/water nanofluids as working fluid in an abandoned oil well to improve thermal performance in the seawater desalination process. *Journal of the Taiwan Institute of Chemical Engineers,* 144, 104754. https://doi.org/10.1016/j.jtice.2023.104754

[21]. Parveez, M., & Hanief, M. (2022). Enhancement of heat transfer in helical coil heat exchangers using nanofluids. *Chemical and Process Engineering,* 43(2), 279–283.

[22]. Naseema, Nawazish Mehdi, S., Manzoor Hussain, M., Bashad, S. K., & Samade, M. A. (2018). Heat enhancement of heat exchanger using aluminium oxide and copper oxide nanofluids with different concentrations. *Materials Today: Proceedings,* 5(2), 6481–6488. https://doi.org/10.1016/j.matpr.2017.12.261

[23]. Belaghit, M., & Saim, R. (2024). Enhancing geothermal wellbore heat exchanger performance through rectangular protrusion integration in repurposed abandoned oil wells. *International Journal of Heat and Technology,* 42(1), 201–209. https://doi.org/10.18280/ijht.420121

[24]. Esfe, M. H., & Togharie, D. (2024). Experimental, price-performance and artificial neural network analysis of MWCNT–CuO/water–EG (50–50) nanofluid as a coolant/antifreeze working fluid. *Korean Journal of Chemical Engineering,* 41(6), 1679–1689. https://doi.org/10.1007/s11814-024-00173-7

[25]. Akarken, G., Cengiz, U., & Bektaş, T. E. (2024). Hydrothermal synthesis of CuO nanoparticles: Tailoring morphology and particle size variations for enhanced properties. *Journal of Advanced Research in Natural and Applied Sciences,* 10(2), 329–336. https://doi.org/10.28979/jarnas.1405595

[26]. Phiwdang, K., Suphankij, S., Mekprasart, W., & Pecharapa, W. (2013). Synthesis of CuO nanoparticles by precipitation method using different precursors. *In Proceedings of the 10th Eco-Energy and Materials Science and Engineering Symposium* (pp. 740–745). https://doi.org/10.1016/j.egypro.2013.06.80827.

[27]. Verma, N., & Kumar, N. (2019). Synthesis and biomedical applications of copper oxide nanoparticles: An expanding horizon. *ACS Biomaterials Science & Engineering,* 5(3), 1170–1188. https://doi.org/10.1021/acsbiomaterials.8b01092

[28]. Kayani, Z. N., Umer, M., Riaz, S., & Naseem, S. (2015). Characterization of copper oxide nanoparticles fabricated by the sol–gel method. *Journal of Electronic Materials,* 44(10), 3704–3709. https://doi.org/10.1007/s11664-015-3867-5